AJNR

Diffusion Tensor MR Imaging in Diffuse Axonal Injury

Konstantinos Arfanakis, Victor M. Haughton, John D. Carew, Baxter P. Rogers, Robert J. Dempsey and M. Elizabeth Meyerand

AJNR Am J Neuroradiol 2002, 23 (5) 794-802
http://www.ajnr.org/content/23/5/794

AJNR Am J Neuroradiol 23:794–802, May 2002

Diffusion Tensor MR Imaging in Diffuse Axonal Injury

Konstantinos Arfanakis, Victor M. Haughton, John D. Carew, Baxter P. Rogers, Robert J. Dempsey, and M. Elizabeth Meyerand

BACKGROUND AND PURPOSE: **Disruption of the cytoskeletal network and axonal membranes characterizes diffuse axonal injury (DAI) in the first few hours after traumatic brain injury. Histologic abnormalities seen in DAI hypothetically decrease the diffusion along axons and increase the diffusion in directions perpendicular to them. DAI therefore is hypothetically associated in the short term with decreased diffusion anisotropy. We tested this hypothesis by measuring the diffusion characteristics of traumatized brain tissue with use of diffusion tensor MR imaging.**

METHODS: **Five patients with mild traumatic brain injuries and 10 control subjects were studied with CT, conventional MR imaging, and diffusion tensor imaging. All patients were examined within 24 hours of injury. In each participant, diffusion tensor indices from homologous normal-appearing white matter regions of both hemispheres were compared. These indices were also compared between homologous regions of each patient and the control group. In two patients, diffusion tensor images from the immediate posttrauma period were compared with those at 1 month follow-up.**

RESULTS: **Patients displayed significant reduction of diffusion anisotropy in several regions compared with the homologous ones in the contralateral hemisphere. Such differences were not observed in the control subjects. Significant reduction of diffusion anisotropy was also detected when diffusion tensor results from the patients were compared with those of the controls. This reduction was often less evident 1 month after injury.**

CONCLUSION: **White matter regions with reduced anisotropy are detected in the first 24 hours after traumatic brain injury. Therefore, diffusion tensor imaging may be a powerful technique for in vivo detection of DAI.**

Traumatic brain injury is a major public health problem, with about 2 million new cases reported in the United States each year (1). Most of these cases are classified as mild. However, approximately 30% of patients with the mild form experience some degree of residual neurologic or cognitive deficit (2). Common symptoms include deficit in attention, working memory, and speed of information processing; headaches; dizziness; and irritability. Diffuse axonal injury (DAI) is widely believed to account for these persistent problems (3–5).

Experimental studies have demonstrated that diffuse white matter injuries may occur with traumatic brain injury irrespective of skull deformation (6). The mechanism for DAI is shear-strain deformation, a change in shape of the brain without a change in volume. Pathology studies have shown that DAI is characterized by multifocal lesions, scattered in white matter, that are occasionally associated with petechial hemorrhage (7). The three areas most commonly involved in DAI are the subcortical white matter, corpus callosum, and dorsolateral aspect of the upper brain stem. From a histologic aspect, several investigators (8–12) have linked DAI to focal misalignments of the cytoskeletal network or to changes of the axolemmal permeability, depending on the severity of the injury. In humans with mild traumatic brain injury, the first evidence of DAI is believed to be focal neurofilament misalignment, which becomes striking within the first 6 hours after injury (Fig 1) (8–11). This misalignment leads to an impairment of axoplasmic transport and local accumulation of organelles. The effect continues for several hours after injury, causing local swelling and expansion of the axonal cylinder (Fig 1). Over time, lobulation of the focal axonal swelling takes place, followed by disconnection of the axon at 30–60 hours after injury. After disconnection, the proximal and distal segments of the axon

Received June 5, 2001; accepted after revision October 22.

From the Departments of Medical Physics (K.A., B.P.R., M.E.M.), Radiology (V.M.H.), Statistics (J.D.C.), and Neurosurgery (R.J.D.), University of Wisconsin, Madison.

Address reprint requests to Konstantinos Arfanakis, PhD, University of Wisconsin, 1530 Medical Science Center, 1300 University Ave, Madison, WI 53706-1532.

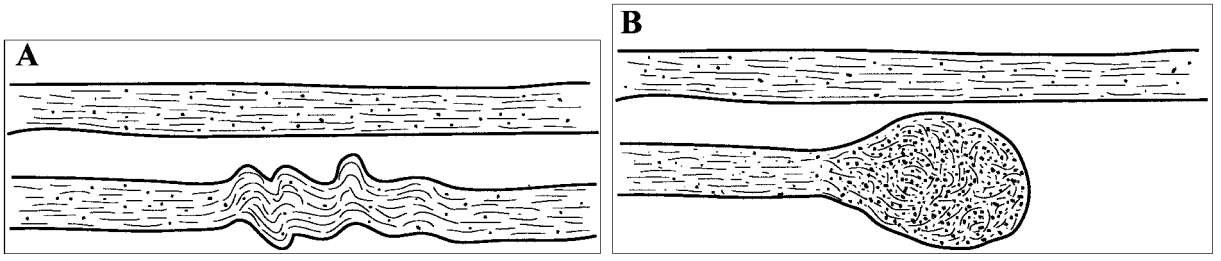

FIG 1. Illustration of the changes that axons undergo owing to cytoskeletal perturbation from mild traumatic brain injury.
A, The top neuron is healthy. In the bottom neuron, neurofilamentous and, generally, cytoskeletal misalignment is visible a short time after injury. This impairs axonal transport.
B, Organelles accumulate in the injured region, causing the axon to swell locally and subsequently disconnect from the rest. In this Figure, the dimensions of the axons relative to the interaxonal space do not necessarily correspond to reality.

become sealed by a continuous axolemma and encompassed by an independent myelin sheath. A study using the tracer horseradish peroxidase determined that axolemmal permeability is not altered after mild traumatic brain injury (11). In moderate and severe traumatic brain injury, however, a change in the axolemmal permeability is the first evidence of injury. After several hours, the neurofilaments become misaligned, leading to local swelling and disconnection (8, 11). Similar findings of focal axoplasmic impairment and swelling have been obtained in several different models of traumatic brain injury (13–15). The only disparity has been that in animals the same events occur much faster than in humans (9). In the most severe form of traumatic brain injury, in addition to the effects just described, direct renting of the axolemma may also occur (8).

Although the widely used Glasgow Coma Scale has excellent interobserver reliability and correlation with outcome following severe brain injury (16), it fails to differentiate between different types of injury with different prognoses and fails to localize the injury. CT or especially MR imaging, however, successfully demonstrates intracranial hematomas, subdural fluid collections, subarachnoid bleedings, cerebral edemas, and degenerating neurons (2, 17–21). Sufficient evidence exists that DAI is not a phenomenon secondary to edema, but occurs as a primary response to trauma (22). In addition, in DAI, not all lesions are associated with hemorrhage. Moreover, degenerating neurons are not present until several days after traumatic brain injury. Therefore, none of these techniques are appropriate imaging tools for DAI.

A more recent noninvasive imaging technique, diffusion tensor imaging, as implemented in MR imaging (23, 24), can be used to probe, in vivo, the intrinsic diffusion properties of deep tissues. Diffusion tensor imaging has been applied in several studies to infer the microstructural characteristics of the brain (25, 26), the heart (27), and the spinal cord (28). In addition, diffusion tensor imaging has been introduced in the diagnosis of disease conditions such as cerebral ischemia (29), acute stroke (30), and multiple sclerosis (31). Unlike conventional diffusion-weighted imaging (32), where diffusion-weighted images are used to calculate the scalar apparent diffusion coefficient, diffusion tensor imaging characterizes diffusive transport of water by an effective diffusion tensor **D**. The eigenvalues of **D** are the three principal diffusivities, and the eigenvectors define the local fiber tract direction field (23). Moreover, one can derive from **D** rotationally invariant scalar quantities that describe the intrinsic diffusion properties of the tissue. The most commonly used are the trace of the tensor (23, 25, 33), which measures mean diffusivity, and fractional anisotropy (FA) and lattice index (LI) (25, 33–35), which characterize the anisotropy of the fiber structure, meaning how much higher the diffusivity is along some directions compared with others.

The purpose of this study was to test the hypothesis that the histologic effects of DAI may be directly detected by means of diffusion tensor imaging in the first hours after injury, through a reduction of the axonal diffusion anisotropy. More specifically, we tested the possibility of using diffusion tensor imaging to detect DAI in patients with traumatic brain injury, by studying white matter regions that appeared normal on CT and other MR images, including apparent diffusion coefficient maps. We compared diffusion tensor imaging results between contralateral homologous structures of each subject and also between homologous structures of each patient and the control group. Finally, in the same normal-appearing white matter regions, we compared diffusion tensor imaging results in the first 24 hours after injury and in a follow-up study 30 days later.

Methods

Participants

This study included five patients with mild traumatic brain injury (three men and two women) and 10 volunteers with no known neurologic disorders (five men and five women). The mean age for the group of patients was 35.6 years (SD = 14.8 years), and for the control group 28.9 years (SD = 7.6 years). All patients were enrolled and studied as soon after admission to the emergency department as possible, but not after 24 hours. Inclusion criteria for the study were a history of recent head trauma that exposed the patient to rapid acceleration or deceleration; symptoms such as amnesia, disorientation, or confusion; a Glasgow Coma Scale score between 13 and 15; and the presence of a relative who could provide informed consent for the MR study. Exclusion criteria were evidence of large intracerebral hematomas, subdural hematomas, or herniations; an indication for immediate surgical treatment of the head injury or other injury; an inability to cooperate with the

examination; and dental devices or other causes for degraded echo planar MR images or a contraindication for MR examination. All participants or the legal guardian signed an informed consent form in accordance with institutional policy.

Image Acquisition

CT scans were obtained in all patients. MR images were acquired in all patients and control subjects with use of a clinical 1.5-T imager with high-speed gradients (40 mT/m maximum amplitude, 150 mT/m/msec slew rate). The following conventional MR sequences were performed during each imaging session: 2D sagittal T1-weighted spin-echo localizer (500/8/1 [TR/TE/excitations], 90° flip angle, 24 × 24-cm field of view [FOV], 256 × 256 imaging matrix, 20 sections, 5-mm section thickness with 1.5-mm skip); 2D axial T2-weighted multiplanar prepared gradient-recalled acquisition in the steady state (800/25/1, 20° flip angle, 22 × 22-cm FOV, 256 × 256 imaging matrix, 23 sections, 5-mm section thickness with 2-mm skip); and 2D axial T1-weighted spin-echo (500/8/1, 90° flip angle, 24 × 24-cm FOV, 256 × 256 imaging matrix, 20 sections, 5-mm section thickness with 1.5-mm skip). Diffusion tensor imaging was performed with a modified 2D spin-echo sequence, with an echo planar imaging acquisition window and a pair of diffusion gradients symmetrically positioned around the 180° radio-frequency pulse. The imaging parameters were 4500/71.8/1, 24 × 24-cm FOV, 21 contiguous sections, 3-mm section thickness. The amplitude of the total diffusion gradient was 40 mT/m and was applied in 23 noncollinear directions uniformly distributed in 3D space. The duration of each diffusion-weighted gradient lobe was 21.3 ms, and their temporal spacing was 26.9 ms. The effective diffusion weighting was $b = 1001$ s/mm^2 (23). To estimate the diffusion tensor for all voxels, T2-weighted images with no diffusion weighting ($b = 0$ s/mm^2) (24) were also acquired at the beginning of each diffusion tensor imaging study. Echo planar readout was performed with a 128 × 128 image matrix, and all images were reconstructed to a 256 × 256 matrix after zero filling. Therefore, the resultant voxel dimensions were 0.9375 × 0.9375 × 3 mm^3. All diffusion tensor images ($b = 0$ s/mm^2 and $b = 1001$ s/mm^2) were acquired four times. The duration of diffusion tensor imaging was 7 minutes 12 seconds, and total imaging time for each subject was less than 15 minutes.

MR imaging and CT examinations were completed for all patients within the first 24 hours after injury. A second diffusion tensor imaging examination was performed in two of the patients 30 days after injury.

Postprocessing

All MR images were transferred to an offline workstation for postprocessing. The four repetitions of the images that were acquired with the diffusion tensor sequence were first averaged to increase the signal-to-noise ratio. Then, for the T2-weighted images with no diffusion weighting, a threshold was selected to remove CSF, and the averaged diffusion-weighted images were registered to these T2-weighted images to correct for distortions induced by eddy currents (36), by using a 2D perspective eight-parameter registration algorithm (37). Next, the diffusion tensor **D** and its eigenvalues and eigenvectors were estimated for all voxels (23). After sorting the eigenvalues in order of decreasing magnitude for each voxel, ($\lambda_1 > \lambda_2 > \lambda_3$), λ_1 represented the diffusivity along the primary diffusion direction ϵ_1 (23). In theory, the primary diffusion direction in a voxel coincides with the mean of the unit vectors that are parallel to the physical axes of the neurons included in that voxel. The second and third largest eigenvalues (λ_2, λ_3) represented the diffusivities along directions that were perpendicular to the primary diffusion direction, and to each other (23). The corresponding eigenvectors (ϵ_2, ϵ_3) represented those secondary diffusion axes. Several diffusion tensor imaging indices were also derived from the eigenvalues and eigenvectors in each voxel. One of these quantities is the trace of the diffusion tensor (23, 25, 33), which is a measure of the mean diffusivity. Diffusion anisotropy, which expresses the degree of selective diffusion along specific directions, was also measured, by means of FA and LI (25, 33–35). According to the definition of LI and FA, measurements of LI are characterized by a lower standard deviation than those of FA but are more susceptible to partial volume effects. Maps of trace, FA, and LI were constructed for all participants.

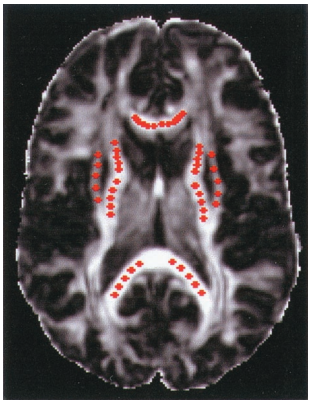

FIG 2. Example of the selection of voxels from the five structures under study, in one section of a control subject. The background image is an LI map. The red dots correspond to the selected voxels. The dots were made larger than the in-plane dimensions of a single voxel for visualization purposes.

A series of voxels was selected systematically in the left and right sides of the external capsule, posterior corpus callosum, anterior corpus callosum, posterior limb of the internal capsule, and anterior limb of the internal capsule in all subjects (Fig 2). For the patients with traumatic brain injury, these voxels were always selected from white matter that appeared normal on conventional MR images, even on trace maps. The selection was performed based on LI maps where the structures were easily identified. Since it was not trivial to detect the border between the posterior and the anterior limbs of the internal capsule based only on LI maps, where the two structures appear to be continuous, absolute value color maps (38) were also produced for all subjects (Fig 3). In these maps, different colors represent specific directions in 3D space, and the intensity at each voxel is weighted by its LI value. The difference between the orientation of neurons in the posterior and the anterior limb of the internal capsule is such that the corresponding colors are also significantly different, therefore simplifying the selection of the voxels (Fig 3). The same rules of voxel selection were applied to all patients and neurologically normal volunteers.

Each side (left, right) of the five aforementioned structures was considered as a separate region of interest (ROI). Fifteen noncontiguous voxels were selected from each ROI. A total of 150 voxels (15 voxels × 5 structures × 2 hemispheres) were chosen in each participant. The selection was performed according to the following protocol. Since thin sections (3 mm) were used for diffusion tensor imaging, portions of each ROI appeared in more than three sections. After identifying all the sections that contained each ROI, voxels from the three central ones were selected. In each one of these three sections, five noncontiguous voxels were selected per ROI. The voxels were evenly spaced from each other within the same section and ROI (Fig 2). Mean λ_1, λ_2, λ_3, trace, FA, and LI and their standard deviations were calculated for each ROI in both hemispheres in all participants.

The diffusion tensor imaging results from each structure in one hemisphere of the brain were compared with those from the contralateral hemisphere for all participants. In addition, the diffusion tensor imaging indices from each patient's ROIs

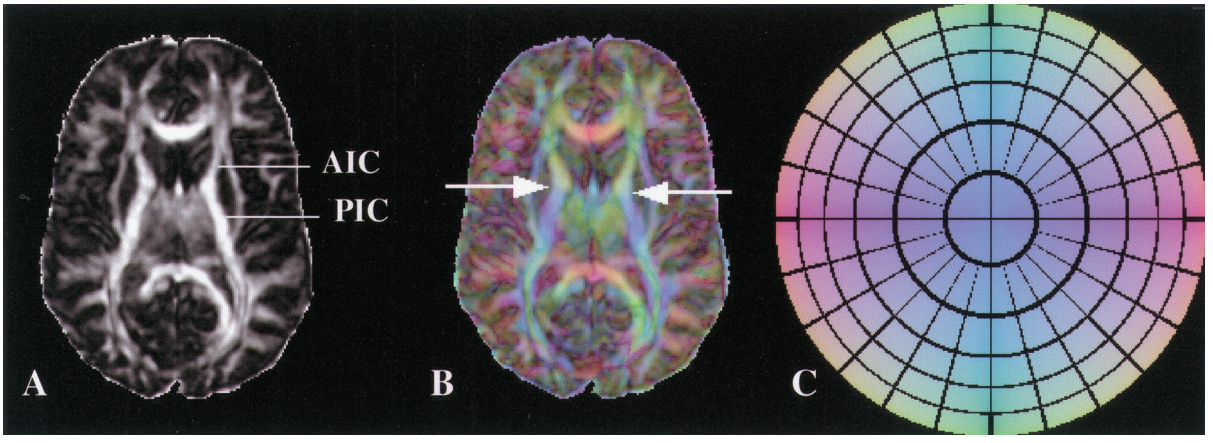

FIG 3. *A*, LI map in a control subject. The border between the anterior (*AIC*) and posterior (*PIC*) limbs of the internal capsule is not obvious from this image.

B, Absolute value color map of the same section as in *A*. *Arrows* indicate the exact level of the border between AIC and PIC. Color representation of directions in 3D space helps to clearly separate the two structures.

C, Color circle demonstrates the correspondence of colors and directions in 3D space. This circle should be thought of as a 3D dome that is viewed from below.

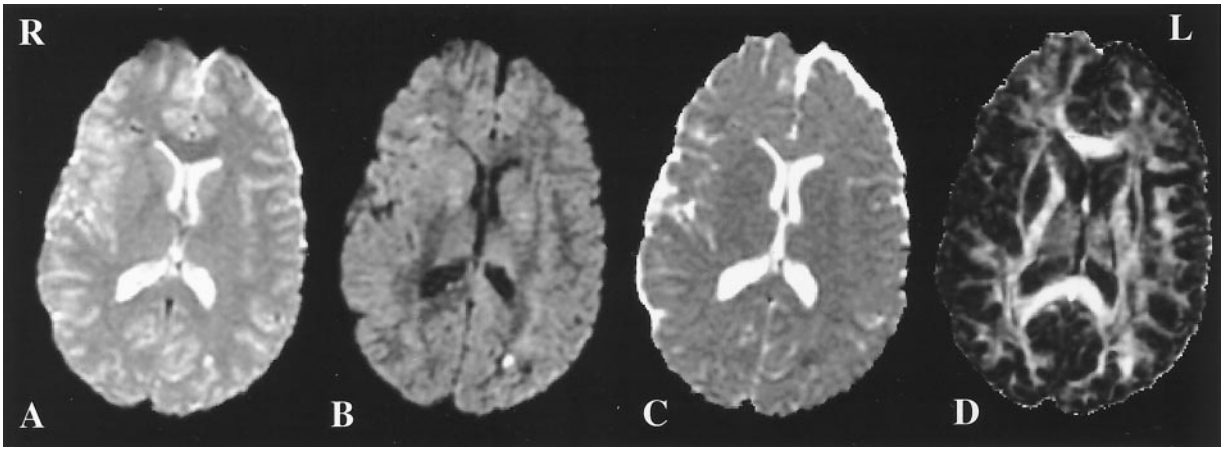

FIG 4. *A*, T2-weighted image in a patient with mild traumatic brain injury. Small hemorrhagic lesions are visible in the left occipital lobe and right frontal lobe.

B, Diffusion-weighted map of the same section in the same patient, for one of the 23 diffusion-weighted gradient directions. The abnormal regions from *A* are also visible in *B*.

C, Corresponding trace map. The same lesions from *A* and *B* can be detected.

D, LI map of the same section in the same patient. Decreased anisotropy is visible in the left internal capsule and left anterior corpus callosum. No abnormality was demonstrated in these regions with any other type of imaging. On this LI map, however, the hemorrhagic lesions from *A*, *B*, and *C* are hard to identify. *R* indicates right; *L*, left.

were compared with those of the control group. The significance of any differences was assessed based on the assumption that the results from the control group were normally distributed. For all structures, values of diffusion tensor indices from the patients were indicated on graphs of the corresponding normal probability densities of the control group. Comparisons were also performed between the results from immediate (<1 day after injury) and short-term follow-up (30 days after injury) diffusion tensor images for two of the patients. For each selected structure, the side with the lower anisotropy on the immediate image was determined. Ratios of several diffusion characteristics between the ROIs with low anisotropy on the immediate image and their homologous contralateral ROIs with higher anisotropy were plotted for the immediate and follow-up data sets. A Student's *t* test was used to determine the statistical significance of the differences between hemispheres and between the immediate and follow-up data sets. A *P* value less than .05 was considered to indicate a statistically significant difference.

Results

For all patients, CT images exhibited no abnormalities. Conventional MR images, especially T2-weighted, and diffusion-weighted images and trace maps demonstrated scattered sites of abnormal signal intensity consistent with petechial hemorrhage or edema. In addition, for all patients, images of diffusion anisotropy (FA, LI) obtained with diffusion tensor imaging revealed regions of reduced anisotropy, differing from the hemorrhagic and edematous lesions (Fig. 4). These regions did not appear to be abnormal on the other types of images. However, anisotropy maps did not often provide sufficient contrast for detection of hemorrhages and edema, where anisotropy values might be similar to those in CSF or gray matter.

Interhemispheric comparisons of diffusion charac-

Diffusion characteristics of five structures from both hemispheres in a patient with mild traumatic brain injury and a healthy control subject

Structure and Parameters	Patient			Control Subject		
	Left Hemisphere	Right Hemisphere	*P* Value	Left Hemisphere	Right Hemisphere	*P* Value
Anterior corpus callosum						
λ_1	1.50 ± 0.15	1.81 ± 0.25	<0.005	1.84 ± 0.27	1.88 ± 0.21	<0.4
λ_2	0.67 ± 0.12	0.45 ± 0.11	<0.005	0.43 ± 0.12	0.42 ± 0.09	<0.4
λ_3	0.37 ± 0.11	0.29 ± 0.08	<0.005	0.20 ± 0.07	0.22 ± 0.07	<0.3
Trace	2.54 ± 0.21	2.55 ± 0.21	≈1	2.46 ± 0.21	2.52 ± 0.23	<0.3
FA	0.6 ± 0.09	0.76 ± 0.09	<0.005	0.80 ± 0.08	0.81 ± 0.06	<0.4
LI	0.47 ± 0.10	0.65 ± 0.1	<0.005	0.72 ± 0.11	0.72 ± 0.07	<1
Posterior corpus callosum						
λ_1	1.74 ± 0.27	1.64 ± 0.22	<0.2	1.71 ± 0.12	1.62 ± 0.14	<0.05
λ_2	0.47 ± 0.15	0.49 ± 0.12	<0.4	0.47 ± 0.10	0.45 ± 0.11	<0.4
λ_3	0.27 ± 0.10	0.24 ± 0.07	<0.2	0.23 ± 0.08	0.16 ± 0.09	<0.025
Trace	2.49 ± 0.25	2.36 ± 0.19	<0.1	2.41 ± 0.15	2.23 ± 0.19	<0.005
FA	0.75 ± 0.10	0.74 ± 0.08	<0.4	0.77 ± 0.07	0.79 ± 0.07	<0.3
LI	0.65 ± 0.12	0.65 ± 0.09	<1	0.69 ± 0.08	0.70 ± 0.08	<0.4
External capsule						
λ_1	1.28 ± 0.13	1.13 ± 0.13	<0.005	1.26 ± 0.12	1.25 ± 0.11	<0.5
λ_2	0.69 ± 0.10	0.73 ± 0.10	<0.1	0.65 ± 0.11	0.66 ± 0.08	<0.4
λ_3	0.37 ± 0.14	0.50 ± 0.10	<0.005	0.34 ± 0.10	0.37 ± 0.05	<0.2
Trace	2.34 ± 0.14	2.36 ± 0.16	<0.4	2.26 ± 0.19	2.28 ± 0.12	<0.4
FA	0.53 ± 0.10	0.39 ± 0.10	<0.005	0.56 ± 0.08	0.53 ± 0.06	<0.2
LI	0.38 ± 0.09	0.26 ± 0.08	<0.005	0.41 ± 0.08	0.37 ± 0.06	<0.1
Posterior internal capsule						
λ_1	1.23 ± 0.17	1.30 ± 0.16	<0.1	1.42 ± 0.11	1.41 ± 0.12	<0.5
λ_2	0.64 ± 0.07	0.54 ± 0.11	<0.005	0.49 ± 0.08	0.46 ± 0.07	<0.2
λ_3	0.36 ± 0.08	0.31 ± 0.04	<0.01	0.25 ± 0.04	0.24 ± 0.07	<0.4
Trace	2.24 ± 0.17	2.14 ± 0.13	<0.025	2.16 ± 0.09	2.12 ± 0.15	<0.2
FA	0.53 ± 0.09	0.63 ± 0.08	<0.005	0.70 ± 0.06	0.71 ± 0.07	<0.4
LI	0.41 ± 0.09	0.50 ± 0.08	<0.005	0.59 ± 0.06	0.60 ± 0.07	<0.4
Anterior internal capsule						
λ_1	1.24 ± 0.13	1.47 ± 0.06	<0.005	1.38 ± 0.15	1.55 ± 0.23	<0.025
λ_2	0.59 ± 0.09	0.50 ± 0.09	<0.01	0.56 ± 0.10	0.52 ± 0.10	<0.2
λ_3	0.42 ± 0.08	0.31 ± 0.06	<0.005	0.33 ± 0.09	0.35 ± 0.10	<0.3
Trace	2.25 ± 0.13	2.29 ± 0.12	<0.2	2.26 ± 0.24	2.41 ± 0.29	<0.1
FA	0.52 ± 0.09	0.68 ± 0.06	<0.005	0.63 ± 0.05	0.67 ± 0.09	<0.1
LI	0.38 ± 0.09	0.56 ± 0.06	<0.005	0.51 ± 0.06	0.55 ± 0.10	<0.1

Note.—Data are the mean ± SD. The values of λ_1, λ_2, λ_3, and trace were multiplied by 10^3 before they were included in the table and are in mm^2/s.

teristics from the five selected structures in all neurologically normal control subjects showed no significant differences in anisotropy (Table). In two control subjects, a part of a selected structure in one hemisphere was characterized by a trace significantly higher ($P < .005$) than the trace of the homologous contralateral region. In all patients, significant differences ($P < .005$) were detected between the mean anisotropy of voxels selected from the two contralateral sides of several structures. The regions with reduced anisotropy were always characterized by a decrease in λ_1 and an increase in λ_2 and λ_3. However, in approximately 95% of the interhemispheric comparisons that were performed in the selected structures of the patients, and that resulted in significantly different anisotropy between the two sides, no significant differences in the trace were detected.

In many of the selected ROIs in each patient, anisotropy was significantly decreased with respect to the mean anisotropy in homologous ROIs in the control group ($P < .05$). No significant differences were observed between the trace values from homologous ROIs of each patient and the controls. However, ROIs with reduced anisotropy, compared with that in the control group, also exhibited reduced λ_1 and increased λ_2 and λ_3. Plotting the diffusion tensor imaging results for the patients on graphs of the corresponding distributions for the control subjects clearly demonstrated these observations (Fig 5). Significant reduction of anisotropy was more often detected in the internal capsule and corpus callosum and less often in the external capsule of the patients with mild traumatic brain injury.

Comparison of diffusion tensor imaging results obtained within 1 day and at 30 days after injury in two patients revealed significant changes in anisotropy in seven ROIs of both patients. In these ROIs, anisotropy values that were found to be lower than normal in the first data set were increased in the second. The corresponding trace values did not change between acquisitions, whereas λ_1 increased and λ_2 and λ_3 decreased. Plots of ratios of the diffusion characteristics between these seven ROIs and their homologous contralateral ones, in the immediate and follow-up data

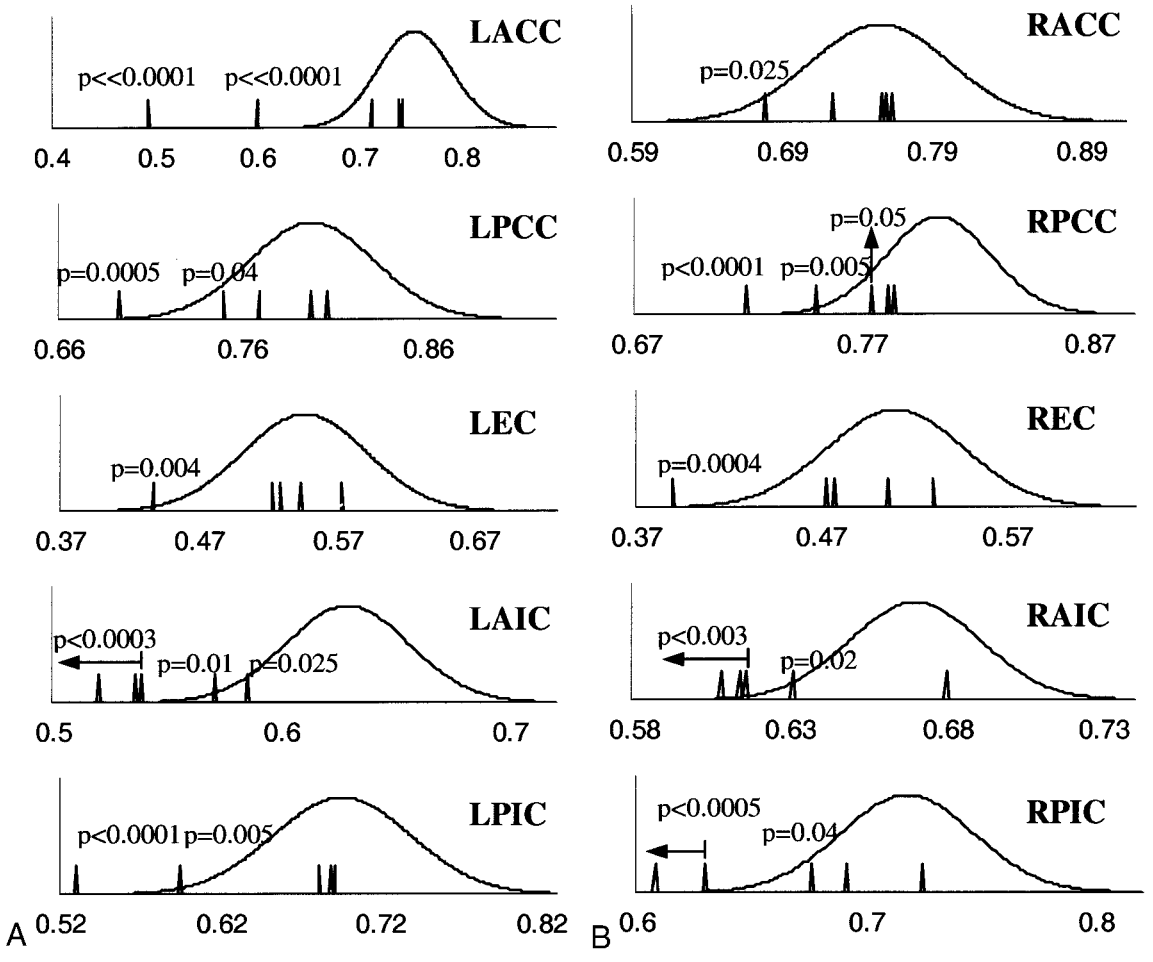

FIG 5. Graphs show distributions of FA results from 10 selected ROIs (5 structures x 2 hemispheres) for the control subjects (continuous lines) combined with the corresponding FA values for the five patients with mild traumatic brain injuries (vertical lines), in the left (*A*) and right (*B*) hemispheres. All horizontal axes represent FA values. *P* values are reported only for cases in which FA results for the patients were significantly different ($P < .05$) from the mean FA results of the control subjects. For the patients, anisotropy was found to be significantly reduced in several structures compared with normal values. Reduction of FA was more often in the internal capsule and corpus callosum and less often in the external capsule of the patients. *LACC* and *RACC* indicate left and right anterior corpus callosum, respectively; *LPCC* and *RPCC*, left and right posterior corpus callosum; *LEC* and *REC*, left and right external capsule; *LAIC* and *RAIC*, left and right anterior internal capsule; *LPIC* and *RPIC*, left and right posterior internal capsule.

sets, demonstrated the temporal nature of the effects of mild traumatic brain injury on white matter (Fig 6). However, although the diffusion properties of these seven ROIs on the second image were more similar to normal, three of them were still characterized by anisotropy values and eigenvalues that were significantly different than normal, and four had reached "normal" diffusion characteristics ($P > .05$). In two ROIs with reduced anisotropy on the first diffusion tensor dataset, no significant change was observed 30 days later.

Discussion

Identification of DAI has been possible after death with invasive histopathologic studies. Electron microscopy, light microscopy, and immunocytochemical methods have been applied in excised human, or animal, brain samples after traumatic brain injury in order to visualize DAI (39, 9, 40). MR imaging, with its ability to differentiate between various types of brain tissue in healthy or diseased conditions, has provided useful information about regions with lesions, such as edema and hemorrhage, following traumatic brain injury. However, conventional MR imaging underestimates the extent of DAI, which may account for much of the transient clinical pathologic conditions following traumatic brain injury and perhaps for the residual neurologic and cognitive deficits that are associated with traumatic brain injury. In this study, we tested the hypothesis that a relatively new MR imaging technique, diffusion tensor imaging, could be more effective in identifying the effects of DAI in vivo.

Images of FA and LI, as well as quantitative comparison of the diffusion characteristics of selected groups of voxels, demonstrated significant differences of diffusion anisotropy between the two sides (left, right) of several white matter structures in the patients. The same was not true in the neurologically normal control subjects. Therefore, regions with reduced anisotropy, compared with their contralateral homologous regions, may be possible sites of DAI.

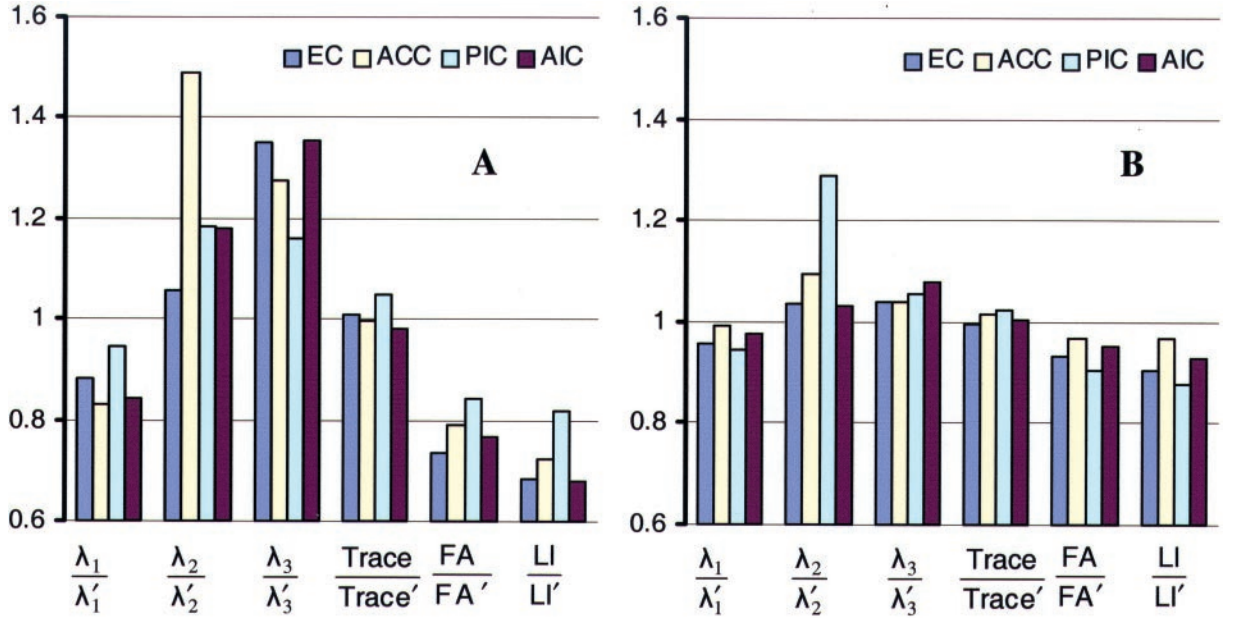

FIG 6. Bar graphs of ratios of diffusion characteristics between the two sides of four structures in a patient with mild traumatic brain injury, using the immediate (*A*) and short-term follow-up (*B*) data. The quantities λ_1, λ_2, λ_3, trace, FA, and LI correspond to that side of the structure that has the lowest anisotropy on the immediate image. The quantities λ_1', λ_2', λ_3', trace', FA', and LI' correspond to the contralateral side of these structures. The four structures are external capsule (*EC*), anterior corpus callosum (*ACC*), posterior internal capsule (*PIC*), and anterior internal capsule (*AIC*). Each structure corresponds to a specific color. For the immediate data set, one side of the four structures has lower λ_1, higher λ_2 and λ_3, and lower FA and LI than its contralateral homologous side. Also, trace is similar for both sides. For the follow-up data set, λ_1, λ_2, λ_3, FA, and LI have become more similar between the two sides of each structure, therefore giving ratios that are closer to 1. The ratios of the trace have remained at values almost equal to 1. When looking at the absolute values of the diffusion characteristics, we notice that the ratios change because the side of each structure that had low anisotropy on the immediate dataset has higher anisotropy on the follow-up dataset.

Although similar changes of anisotropy could be caused by edema or hemorrhage, there was no indication for the presence of such lesions on any CT or MR image. Furthermore, diffusivity values were not altered in the same regions. These results support the hypothesis that DAI may be detected by means of reductions in diffusion anisotropy. They may also explain why conventional diffusion-weighted imaging studies have not effectively detected DAI by using only measures of mean diffusivity (21).

In the patients, several regions were characterized by significantly lower diffusion anisotropy compared with the mean values from the control group. There was no indication for the presence of edema or hemorrhage in these regions. Although for several structures anisotropy values were abnormal, trace or mean diffusivity was not significantly different than the corresponding mean values for the control group. This observation also confirmed that our choice to study patients with mild traumatic brain injury by means of diffusion anisotropy instead of mean diffusivity was advantageous.

To understand how DAI may cause changes in the diffusion anisotropy values of white matter, one has to carefully study the results from histologic studies. Several researchers agree that the first indication of DAI in patients with mild traumatic brain injury is a misalignment of the cytoskeletal network (Fig 1A) (8–12). In addition, at low b values, similar to the ones used in our study, diffusion measurements are mostly sensitive to the extraaxonal space (41). Therefore, diffusion anisotropy in white matter is due to the fact that diffusion is more impeded perpendicularly to the fibers mainly because of their geometric arrangement. In DAI, misalignment of the axonal membranes may increase restriction in diffusion parallel to the main axis of the neurons, thus decreasing λ_1. Additionally, misalignment of the cytoskeletal network may possibly increase diffusion in directions perpendicular to the axons due to an additional diffusion component, created by the projection of the primary diffusivity on the transverse plane, therefore increasing λ_2 and λ_3. Consequently, misalignment of the axonal membranes in DAI could be responsible for reductions of anisotropy. The second phase of DAI includes an impairment of axoplasmic transport and local accumulation of organelles, causing local swelling and expansion of the axonal cylinder (Fig 1) (8–12). This change in shape may also increase restriction in the diffusion along the main axis of the fibers and decrease local diffusion anisotropy. Following lobulation, disconnection may occur that might lead to the death of the distal and proximal segments of the neuron (8–12). The membrane of a dying neuron degenerates, thus reducing restriction in diffusion along directions perpendicular to the axon, increasing λ_2 and λ_3, and reducing anisotropy. For moderate and severe traumatic brain injuries, an increase of permeability also takes place in the injured axons (8–12). This may also increase diffusivity in directions perpendicular to the axons and reduce anisotropy. Some of the effects that can happen in DAI

may not have occurred in the patients with mild traumatic brain injury in this study, either due to timing or due to severity of injury. However, all the possible histologic changes that have been associated with DAI may lead to a reduction in diffusion anisotropy through different mechanisms. Although we obtained no pathologic proof that the changes in diffusion anisotropy were associated with DAI, we could find no alternative plausible explanation.

A follow-up study in two patients with mild traumatic brain injury revealed that in some regions with initially reduced diffusion anisotropy the changes were partially, or completely, corrected 30 days after injury. These results should not be interpreted as evidence for regeneration of neurons. Instead, a cellular repair mechanism may have corrected the cytoskeletal misalignment and lobulation, before disconnection occurred. Thus, diffusion anisotropy increased as the axon returned to its original condition. In some cases, 30 days after injury, diffusion anisotropy was no longer different than normal values. This might be due to a complete repair process. In others, diffusion anisotropy was somewhat increased, but still significantly lower than normal. This could be explained with a repair process that was either not completed 30 days after injury, or it was finished and the final condition of the axons was different than their healthy state. Finally, several white matter regions with reduced diffusion anisotropy one day after injury did not exhibit any change 30 days later. In these cases, disconnection might have happened, and Wallerian degeneration of the injured neurons might have occurred.

In a recent study of diffusion tensor imaging in two patients approximately 1 year after severe traumatic brain injury, reduced anisotropy was detected in the internal capsule in one of the patients (42). This was claimed to be due to loss of the parallel fiber arrangement of the major white matter tracts. Although this observation seems to agree with our results, it was acquired at a much later time after severe injury and cannot be easily compared. The same study also reported multiple sites of increased diffusivity in white matter. These data were translated as an expansion of the extracellular space, caused by neuronal or glial cell loss. The fact that we did not observe any changes in mean diffusivity in our study could be due to insufficient time for completion of Wallerian degeneration, or due to minor neuronal loss in connection with the mild injuries (43). Furthermore, the characteristics of the rest of the processes that take place in DAI in patients with mild traumatic brain injury might be such that mean diffusivity would not be significantly affected.

Most of the abnormalities in diffusion anisotropy values were detected in the internal capsule and the corpus callosum in the five patients. These results are in accordance with histology research in traumatic brain injury, which has concluded that the three sites most commonly involved in DAI are the subcortical white matter, the corpus callosum, and the upper brain stem. We did not perform any measurements directly inside the upper brain stem, because additional imging time would have been required to include this structure. However, many axons that cross through that region also belong to the internal capsule. Therefore, it is possible that the changes we observed in the diffusion characteristics of the internal capsule may be related to damage in the upper brain stem.

One of the limitations of our study was that not all of the voxels in the white matter structures under investigation were used. Instead representative voxels were selected from each structure. Although the selection was performed carefully and with very well determined criteria, the process was time-consuming and the results might be somewhat biased. A solution to this problem would be implementation of a segmentation algorithm that would separate several white matter structures. This would allow investigation of more brain regions than those studied here, and also all the voxels in each structure could be accounted for.

An additional limitation of our study is the relatively small number of neurologically normal control subjects that were included. If more control subjects were available, we could have performed age-matched comparisons between the diffusion characteristics of each patient and the corresponding control subgroup. This is important since diffusion anisotropy is inversely proportional to the age of the subject (44). However, our measurements are not significantly affected, since the age of most of our patients was very similar to the mean age of the control subjects. Also, for the patients whose age was much different than the mean for the control subjects, the reduction of anisotropy that may have occurred due to age is much less significant than the changes we observed (44).

For two of the patients, we performed diffusion tensor imaging within 1 day of injury and 30 days after injury. It would be extremely interesting to acquire multiple diffusion tensor imaging data sets at short time intervals starting the first hours after injury. Initially, this might provide useful information about the severity of injury and the sites of DAI. Then a detailed longitudinal study would reveal how DAI progresses in each patient. Finally, after enough experience has been gained, longitudinal DTI studies in multiple patients with traumatic brain injury might provide knowledge that would assist physicians in predicting future changes in white matter that are characterized by DAI. Possible treatments could also be tested.

Moderate and severe traumatic brain injuries demonstrate, in addition to the effects found in the mild form, an increase in the permeability of the axon's membranes (8–12). Although we predicted that such changes would increase diffusivity in directions perpendicular to the axon and decrease diffusion anisotropy, diffusion tensor imaging in such patients is necessary to confirm this hypothesis.

Conclusion

The present study demonstrated that DAI might be detected in patients with mild traumatic brain injury through a reduction of the diffusion anisotropy. Interhemispheric and intersubject comparisons exhibited significant reduction of anisotropy in several white matter structures, early after injury. Most of the DAI sites appeared to be in the internal capsule and the corpus callosum. Furthermore, a follow-up study revealed several regions that might have recovered from the injury 1 month later. The technique presented herein might provide a tool for in vivo detection of DAI at the very early stages in patients with mild traumatic brain injury. This could have significant implications not only for the diagnosis but also for the treatment of these patients.

References

1. Kraus J, Nourjah P. **The epidemiology of mild head injury**. In: Levin H, Eisenberg H, Benton A, eds. *Mild Head Injury.* Oxford: Oxford University Press; 1989:8–22
2. Mittl RJ, Grossman RI, Hiehle JF, et al. **Prevalence of MR evidence of diffuse axonal injury in patients with mild head injury and normal head CT findings**. *AJNR Am J Neuroradiol* 1994;15:1583–1589
3. Capruso DX, Levin HS. **Cognitive impairment following closed head injury**. *Neurol Clin* 1992;10:879–893
4. Evans RW. **The postconcussion syndrome and the sequelae of mild head injury**. *Neurol Clin* 1992;10:815–847
5. Levin HS, Mattis S, Ruff RM, et al. **Neurobehavioral outcome following minor head injury: a three-center study**. *J Neurosurg* 1987;66:234–243
6. Holbourn AHS. **The mechanics of brain injuries**. *Br Med Bull* 1945;3:147–149
7. Adams JH. **Head injury**. In: Adams JH, Corsellis JAN, Duchen LW, eds. *Greenfield's Neuropathology*. 4th ed. New York: John Wiley and Sons; 1984:85–124
8. Povlishock JT, Christman JT. **The pathobiology of traumatically induced axonal injury animals and humans: a review of current thoughts**. *J Neurotrauma* 1995;12:555–564
9. Christman CW, Grady MS, Walker SA, Holloway KL, Povlishock JT. **Ultrastructural studies of diffuse axonal injury in humans**. *J Neurotrauma* 1994;11:173–186
10. Grady MS, McLaughlin MR, Christman CW, Valadka AB, Fligner CL, Povlishock JT. **The use of antibodies targeted against the neurofilament subunits for the detection of diffuse axonal injury in humans**. *J Neuropathol Exp Neurol* 1993;52:143–152
11. Pettus EH, Christman CW, Giebel ML, Povlishock JT. **Traumatically induced altered membrane permeability: its relationship to traumatically induced reactive axonal change**. *J Neurotrauma* 1994; 11:507–522
12. Gennarelli TA. **The pathobiology of traumatic brain injury**. *Neuroscientist* 1997;3:73–81
13. Gennarelli TA, Thibault LE, Tipperman R, et al. **Axonal injury in the optic nerve: a model simulating diffuse axonal injury in the brain.** *J Neurosurg* 1989;71:244–253
14. Maxwell WL, Kansagra AM, Graham DI, Adams JH, Gennarelli TA. **Freeze-fracture studies of reactive myelinated nerve fibers after diffuse axonal injury**. *Acta Neuropathol* 1988;76:395–406
15. Tomei G, Spagnoli D, Ducati A, et al. **Morphology and neurophysiology of focal axonal injury experimentally induced in the guinea pig optic nerve**. *Acta Neuropathol* 1990;80:506–513
16. Ong L, Selladurai BM, Dhillon MK, Atan M, Lye MS. **The prognostic value of the Glasgow Coma Scale, hypoxia and computerized tomography in outcome prediction of pediatric head injury**. *Pediatr Neurosurg* 1996;24:285–291
17. Kelly AB, Zimmerman RD, Snow RB, Gandy SE, Heier LA, Deck MDF. **Head trauma: comparison of MR and CT—experience in 100 patients**. *AJNR Am J Neuroradiol* 1988;9:699–708
18. Friedman SD, Brooks WM, Jung RE, Hart BL, Yeo RA. **Proton MR spectroscopic findings correspond to neuropsychological function in traumatic brain injury**. *AJNR Am J Neuroradiol* 1998;19: 1879–1885
19. Hofman PAM, Stapert SZ, van Kroonenburgh MJPG, Jolles J, de Krujik J, Wilmink JT. **MR imaging, single-photon emission CT, and neurocognitive performance after mild traumatic brain injury**. *AJNR Am J Neuroradiol* 2001;22:441–449
20. Hofman PAM, Kemerink GJ, Jolles J, Wilmink JT. **Quantitative analysis of magnetization transfer images of the brain: effect of closed head injury, age and sex on white matter**. *Magn Reson Med* 1999;42:803–806
21. Liu A, Maldijian J, Bagley L, Sinson G, Grossman R. **Traumatic brain injury: diffusion weighted imaging findings.** *AJNR Am J Neuroradiol* 1999;20:1634–1641
22. Adams JH, Graham DI, Murray LS, Scott G. **Diffuse axonal injury due to nonmissile head injury in humans: an analysis of 45 cases.** *Ann Neurol* 1982;12:557–563
23. Basser PJ, Mattiello J, Le Bihan D. **MR diffusion tensor spectroscopy and imaging**. *Biophys J* 1994;66:259–267
24. Basser PJ, Mattiello J, Le Bihan D. **Estimation of the effective self-diffusion tensor from the NMR spin echo**. *J Magn Reson B* 1994;103:247–254
25. Pierpaoli C, Jezzard P, Basser PJ, Barnett A, Di Chiro G. **Diffusion tensor MR imaging of the human brain**. *Radiology* 1996;201:637–648
26. Virta A, Barnett A, Pierpaoli C. **Visualizing and characterizing white matter fiber structure and architecture in the human pyramidal tract using diffusion tensor MRI**. *Magn Reson Imaging* 1999; 17:1121–1133
27. Holmes AA, Scollan DF, Winslow RL. **Direct histological validation of diffusion tensor MRI in formaldehyde-fixed myocardium**. *Magn Reson Med* 2000;44:157–161
28. Fenyes DA, Narayana PA. **In vivo diffusion tensor imaging of rat spinal cord with echo planar imaging**. *Magn Reson Med* 1999;42: 300–306
29. Lythgoe MF, Busza AL, Calamante F, et al. **Effects of diffusion anisotropy on lesion delineation in a rat model of cerebral ischemia**. *Magn Reson Med* 1997;38:662–668
30. van Gelderen P, de Vleeschouwer MHM, DesPres D, Pekar J, van Zijl PCM, Moonen CTW. **Water diffusion and acute stroke**. *Magn Reson Med* 1994;31:154–163
31. Werring DJ, Clark CA, Barker GJ, Thompson AJ, Miller DH. **Diffusion tensor imaging of lesions and normal-appearing white matter in multiple sclerosis**. *Neurology* 1999;52:1626–1632
32. Le Bihan D. **Diffusion NMR imaging**. *Magn Reson Q* 1991;7:1–30
33. Basser PJ. **Inferring microstructural features and the physiological state of tissues from diffusion-weighted images**. *NMR in Biomedicine* 1995;8:333–344
34. Basser PJ, Pierpaoli C. **Microstructural and physiological features of tissues elucidated by quantitative-diffusion-tensor MRI**. *J Magn Reson B* 1996;111:209–219
35. Pierpaoli C, Basser PJ. **Toward a quantitative assessment of diffusion anisotropy**. *Magn Reson Med* 1996;36:893–906
36. Haselgrove JC, Moore JR. **Correction for distortion of echo-planar images used to calculate the apparent diffusion coefficient**. *Magn Reson Med* 1996;36:960–964
37. Woods RP, Grafton ST, Holmes CJ, Cherry SR, Mazziotta JC. **Automated image registration, I: general methods and intrasubject, intramodality validation**. *J Comp Assist Tomogr* 1998;22:141–154
38. Pajevic S, Pierpaoli C. **Color schemes to represent the orientation of anisotropic tissues from diffusion tensor data: application to white matter fiber tract mapping in the human brain**. *Magn Reson Med* 1999;42:526–540
39. Adams JH. **Head injury**. In: Adams JH, Duchen LW, eds. *Greenfield's Neuropathology*. 5th ed. London: Edward Arnold; 1992:106–152
40. Gentleman SM, Nash MJ, Sweeting CJ, Graham DI, Roberts GW. **β-Amyloid precursor protein (β-APP) as a marker for axonal injury after head injury**. *Neurosci Lett* 1993;160:139–144
41. Le Bihan D, Mangin JF, Poupon C, et al. **Diffusion tensor imaging: concepts and applications**. *J Magn Reson* 2001;13:534–546
42. Rugg-Gunn FJ, Symms MR, Barker GJ, Greenwood R, Duncan JS. **Diffusion imaging shows abnormalities after blunt head trauma when conventional magnetic resonance imaging is normal**. *J Neurol Neurosurg Psychiatry* 2001;70:530–533
43. Gennarelli TA, Thibault LE, Adams JH, Graham DI, Thompson CJ, Marcincin RP. **Diffuse axonal injury and traumatic coma in the primate**. *Ann Neurol* 1982;12:564–574
44. Pfefferbaum A, Sullivan EV, Hedehus M, Lim KO, Adalsteinsson E, Moseley M. **Age-related decline in brain white matter anisotropy measured with spatially corrected echo-planar diffusion tensor imaging**. *Magn Reson Med* 2000;44:259–268